2018

Extracting interface locations in multilayer polymer waveguide films using scanning angle Raman spectroscopy

Jonathan M. Bobbitt
Iowa State University and Ames Laboratory

Emily A. Smith
Iowa State University and Ames Laboratory, esmith1@iastate.edu

Extracting interface locations in multilayer polymer waveguide films using scanning angle Raman spectroscopy

Abstract
There is an increasing demand for nondestructive in situ techniques that measure chemical content, total thickness, and interface locations for multilayer polymer films, and scanning angle (SA) Raman spectroscopy in combination with appropriate data models can provide this information. A SA Raman spectroscopy method was developed to measure the chemical composition of multilayer polymer waveguide films and to extract the location of buried interfaces between polymer layers with 7- to 80-nm axial spatial resolution. The SA Raman method acquires Raman spectra as the incident angle of light upon a prism-coupled thin film is scanned. Six multilayer films consisting of poly(methyl methacrylate)/polystyrene or poly(methyl methacrylate)/polystyrene/poly(methyl methacrylate) were prepared with total thicknesses ranging from 330 to 1,260 nm. The interface locations were varied by altering the individual layer thicknesses between 140 and 680 nm. The Raman amplitude ratio of the 1,605-cm−1 peak for polystyrene and 812-cm−1 peak for poly(methyl methacrylate) was used in calculations of the electric field intensity within the polymer layers to model the SA Raman data and extract the total thickness and interface locations. There is an average 8% and 7% difference in the measured thickness between the SA Raman and profilometry measurements for bilayer and trilayer films, respectively.

Keywords
bilayer and trilayer polymer films, polymer–polymer interface, thin-film analysis, vibrational spectroscopy

Disciplines
Materials Chemistry | Materials Science and Engineering | Polymer and Organic Materials

Extracting Interface Locations in Multilayer Polymer Waveguide Films using Scanning Angle Raman Spectroscopy

Jonathan M. Bobbitt and Emily A. Smith*

The Ames Laboratory, U.S. Department of Energy, and Department of Chemistry, Iowa State University, Ames, IA 50011, United States

**Corresponding Author: ***Email: esmith1@iastate.edu

Abstract

There is an increasing demand for nondestructive *in situ* techniques that measure chemical content, total thickness, and interface locations for multilayer polymer films, and SA Raman spectroscopy in combination with appropriate data models can provide this information. A scanning angle (SA) Raman spectroscopy method was developed to measure the chemical composition of multilayer polymer waveguide films and to extract the location of buried interfaces between polymer layers with 7–80-nm axial spatial resolution. The SA Raman method measures Raman spectra as the incident angle of light upon a prism-coupled thin film is scanned. Six multilayer films consisting of poly(methyl methacrylate)/polystyrene or poly(methyl methacrylate)/polystyrene/poly(methyl methacrylate) were prepared with total thicknesses ranging from 330-1260 nm. The interface locations were varied by altering the individual layer thicknesses between 140-680 nm. The Raman amplitude ratio of the 1605 cm^{-1} peak for PS and

812 cm^{-1} peak for PMMA was used in calculations of the electric field intensity within the polymer layers to model the SA Raman data and extract the total thickness and interface locations. There is an average 8% and 7% difference in the measured thickness between the SA Raman and profilometry measurements for bilayer and trilayer films, respectively.

Keywords: Vibrational spectroscopy, Thin film analysis, Polymer polymer interface, Bilayer and trilayer polymer films

Introduction

Polymer-polymer interface characterization in multilayer polymer films is important for their increasing use in energy storage and capture devices,[1-11] coatings and optics,[12-15] food packaging,[16-18] and biomedical applications.[19] Work on understanding polymer-polymer interface surface mixing,[20] roughness,[21] and stability[22,23] is a focus of many multilayer polymer film studies. As important is characterizing the chemical composition, thickness, and interface locations when creating and optimizing new multilayer polymer devices. Optical-based spectroscopies are well suited for *in situ* nondestructive measurements of polymer films.

Infrared variable angle spectroscopic ellipsometry (IR-VASE) is a technique that is capable of providing multilayer polymer interface and chemical content information.[24] Good signal-to-noise ratio IR-VASE spectra require 8-12 hour collection times for a single multilayer polymer film, which limits the real-time analysis of samples. Infrared spectroscopy operated in attenuated total reflection mode is well suited for monitoring chemical content information during the layer-by-layer formation of polyelectrolyte multilayer films.[25-27] Extracting

thicknesses and buried interface locations from the spectra, however, is complicated due to the penetration depth of evanescent waves varying across the infrared spectrum.

Raman spectroscopy provides chemical content information using a single excitation wavelength. Micro-Raman spectroscopy with epi-illumination can provide chemical content information for thin multilayer polymer films, but does not provide buried interface locations from polymer films under approximately 2 μm.[28-30] Scanning angle (SA) Raman spectroscopy is a technique that couples a sample to a prism (a schematic is shown in the top of Fig. 1), and a data set consist of the Raman spectra as a function of the incident angle of the excitation light. SA Raman spectroscopy has been used to measure polymer waveguide thicknesses, buried bilayer film interfaces, and mixed polymer film chemical composition.[31-34] Other reported methods that are similar to SA Raman spectroscopy, variable-angle internal-reflection and attenuated total reflection Raman spectroscopy, have been used to measure bilayer polymer films.[35,36] These studies focused on micron to hundreds of microns thick bilayer films, the reported methods cannot be easily applied to other polymer systems or, in the work by Fumihiko *et al.*, no buried interface location was extracted.

Summarized here is a nondestructive method that combines SA Raman spectroscopy and electric field calculations to extract total thickness and interface locations for thin bilayer and trilayer polymer waveguide films. Polymer films behave as a waveguide when the thickness is greater than approximately $\frac{\lambda}{2\eta}$, where λ is the excitation wavelength and η is the refractive index of the polymer at the excitation wavelength. When light is coupled into the waveguide through a prism, constructive interference occurs at discrete incident angles (referred to as waveguide mode angles), which produces an enhancement in the Raman signal collected at these angles. Previous work by Meyer *et al.*, used electric field calculations to model SA Raman spectra of

homopolymer waveguides of varying thicknesses.[31] Raman scattering is proportional to the square of the electric field, so SA Raman spectra are modeled by plotting the square of the electric field intensity integrated over the thickness of each polymer layer (*i.e.,* SSEF) as a function of the incident angle. The current work expands the bilayer polymer film work reported by Damin *et al.*[33] in two important ways. First, we apply the SA Raman amplitude ratio between peaks for each polymer in the film, which has been previously proposed by us to measure mixed polymer films,[34] and recursive SSEF calculations to reduce the computational time required to model the SA Raman data. Second, total film thickness and interface locations for bilayer and trilayer polymer films with distinctly different indices of refraction are reported. This new method significantly reduces analysis time and is demonstrated on thin (< 1.3 μm) bilayer poly(methyl methacrylate)/polystyrene (PMMA/PS) and trilayer (PMMA/PS/PMMA) waveguide films with one or two buried interfaces, respectively. The presented method should be applicable to measure numerous polymer multilayer films whenever the layers have at least one distinct Raman peak.

Experimental

Sample preparation

A 31.3 mg/mL PS (192,000 g/mol, Sigma Aldrich, St. Louis, MO), 39.0 mg/mL PMMA (120,000 g/mol, Sigma Aldrich, St. Louis, MO), 55.3 mg/mL PMMA, and 67.9 mg/mL PMMA solutions were prepared from 120 mg/mL stock solutions in toluene (Fisher Scientific, Waltham, MA). The PMMA solutions of varying concentration were used to fabricate PMMA layers with different thicknesses and to change the interface location(s) in the multilayer films. PS and

PMMA films were prepared by spin coating 200 µL of solution with a KW-4A spin coater (Chemat Technology, Northridge, CA) at 3000 rpm for 60 seconds. Glass cover slips (25 mm^2 area, Corning Inc., Corning, NY) and sapphire disks (507 mm^2 area, Meller Optics, Providence, RI) were used as substrates, and the film's total and individual layer thicknesses were measured on an AlphaStep® D-600 stylus profiler (KLA Tencor, Milpitas, CA).

Multilayer films were prepared by using the wedge transfer method.[37] A PS film was lifted off of the sapphire disk and floated at the water-air interface using a beaker of water. The PS film was deposited over a PMMA film and the bilayer was dried at 70 °C for 10 minutes. The bilayer film was then left in a petri dish for 24 hours at room temperature to ensure all the residual water had evaporated. After the PMMA/PS bilayer SA Raman measurements were completed, a second PMMA film was lifted off a sapphire disk using a beaker of water and the second PMMA film was placed on top of the bilayer film to create a PMMA/PS/PMMA trilayer film. The drying process was repeated for the trilayer samples.

Scanning angle Raman measurements

A home-built instrument, previously reported by Lesoine *et al.*, was used to collect SA Raman spectra.[38] A 532-nm excitation source (Coherent, Santa Clara, CA) set to s-polarized light was directed onto a sapphire prism (ISP Optics, Irvington, NY) by coupling the source into a polarization maintaining single mode fiber (Thorlabs, Newton, NJ). The incident angle was controlled by using a rotational stage (Zaber Technologies, Vancouver, British Columbia, Canada), which had the fiber mounted on it with a 28-mW laser output. The SA Raman data were collected over an angle range of 48.0-62.0° with a 0.2° step size. A 0.25 numerical aperture 10× microscope objective (Leica, Wetzlar, Germany) was used to direct the collected SA Raman signal into an optical microscope (Leica, Wetzlar, Germany). The light was focused onto a

HoloSpec $f/1.8$i spectrograph (Kaiser Optical Systems, Ann Arbor, MI) that was attached to the side port of the optical microscope. A Newton 940 charged coupled device (Andor Technology, Belfast, UK) with 2048 × 512 pixels was used to collect the SA Raman spectra for 60s with two replicate measurements at each angle.

Igor Pro 6.36 scientific analysis and graphing software was used to process all SA Raman spectra. A Gaussian function with a linear baseline was used to batch fit and extract the amplitudes of PS and PMMA peaks at 1605 and 812 cm^{-1}, respectively. SA Raman spectra were plotted as a function of their incident angle using Matlab 2016b. The SA Raman amplitude ratio (r_{PS}) was calculated at each incident angle using equation 1, where *I* represents the peak amplitude at the designated wavenumber for the indicated polymer and σ_R is the relative Raman cross-section (defined in equation 2).

$$r_{PS} = \frac{I_{PS,.1605\ cm^{-1}}}{I_{PS,1605\ cm^{-1}} + (I_{PMMA,812\ cm^{-1}} \times \sigma_R)} \quad (1)$$

$$\sigma_R = \frac{I_{PS,1605\ cm^{-1}}}{I_{PMMA,812\ cm^{-1}}} = 1.0 \quad (2)$$

The relative Raman cross-section (σ_R) was determined using epi-illumination with a 532-nm excitation source on a XploRA Plus confocal Raman microscope (Horiba Scientific, Edison, NJ). The samples used to determine σ_R were prepared and characterized as previously reported.[34] The thickness of the samples ensured that the Raman signal was independent of the optical focus (*i.e.*, the same amount of polymer was measured regardless of the focus). Spectra were acquired for 5s with 2 accumulations from 3 separate locations.

Electric field and sum square electric field (SSEF) calculations

Electric field intensity calculations were performed using finite-difference time-domain simulations (EM Explorer, San Francisco, CA). The refractive indices of each polymer layer and the SA Raman amplitude ratio (r_{PS}) were input parameters needed in the calculation to find the thickness of each layer. The refractive index for 532-nm and s-polarized light was 1.764 for sapphire, 1.495 for PMMA, and 1.598 for PS.[39-41] A recursive script (included in the supplemental information) for the finite-difference time-domain calculations varied the total thickness (10-nm step size) over the range shown in Table 1. For a given total thickness, the fractional composition of each polymer was modeled by the SA Raman amplitude ratio (r_{PS}), which was varied in increments of 0.05 over the range of values listed in Table 1. (The range of values in Table 1 represent the experimentally measured range across all incident angles). While the SA Raman amplitude ratio does not match the film composition, as discussed below, over the waveguide mode angle range it can be used to approximate the composition and minimize the computation time required to fit the data. Because the SA Raman amplitude ratio (r_{PS}) range varied for each sample (Table 1), the step size for the thickness of each layer also varied with each sample.

The electric field intensity was calculated over an incident angle range of 48.0-62.0° with a 0.2° step size unless otherwise noted. A 12-nm Yee cell size was used for all calculations. The SSEF was determined by integrating the electric field intensity across the entire thickness of the individual polymer layers. The standard error of the estimate (s_{est}), the square root of the average across all angles squared deviation of the experimental data from the SSEF fit, was calculated for each SSEF fit. The lowest s_{est} value provided the best fit between the experimental data and the SSEF fit. For each polymer film, a SSEF fit was individually determined for the PS and PMMA waveguide modes to determine total thickness and interface

location(s). Then the average of the PS and PMMA values were calculated. The reported uncertainties in the total thickness and interface location(s) were determined by finding the second-best SSEF fit (the second lowest s_{est}) that is shifted by at least 0.2°, the angular resolution for these measurements, from the best fit to the experimental data. The waveguide mode maximum angle for PS and PMMA was determined by fitting the SSEF fit to a Lorentzian function and the standard deviation was determined from the Igor Pro fitting software.

Results and Discussion

Motivation for determining buried interfaces using SA Raman spectroscopy

Understanding how the electric field varies across the thickness of a bilayer or trilayer film, as well as with incident angle, is important for understanding the collected SA Raman signal since the electric field intensity is proportional to the Raman signal. The measured parameters in the SA Raman data (*e.g.*, peak intensities and waveguide mode angles) in combination with electric field calculations are used to extract interface locations from thin bilayer and trilayer polymer waveguide films.

The graph of the electric field intensity across the polymer samples are shown in Fig. 1 for selected bilayer (left) and trilayer (right) films. Hereafter, samples will be referred to with a sample number (1, 2, or 3) and -Bi (for bilayer) or -Tri (for trilayer) films. The electric field profiles shown in Fig. 1 are calculated using the experimentally measured polymer thicknesses for four samples: 1-Bi (Fig. 1A), 2-Bi (Fig. 1B), 1-Tri (Fig. 1C), and 2-Tri (Fig. 1D). All bilayer and trilayer samples are thick enough (≥167 nm) to behave as a waveguide using 532-nm excitation, and clearly show angle-dependent electric field intensities as expected. Sample 1-Bi

has 140 nm of PMMA and 180 nm of PS. Across the angle range of 48.0-62.0° a single waveguide mode is evident, and the waveguide mode angles are at 54.90° and 55.50° for PS and PMMA, respectively. The electric field intensity is generated in both the PMMA and PS layers. However, the electric field intensity distribution varies with the incident angle and does not match the 55% PS polymer composition at all incident angles. For example, 63% of the total electric field intensity is generated in the PS layer at the 54.90° PS waveguide mode angle.

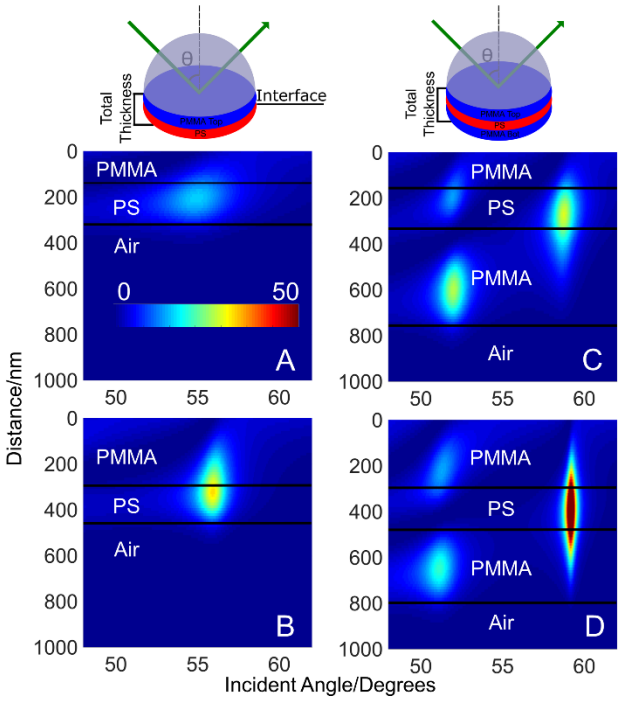

Figure 1: Calculated electric field intensity (square of the electric field) plots as a function of incident angle and distance from the prism/sample interface, which is located at 0 nm. The color scale represents the electric field intensity, and the scale in (A) is the same for all plots. The solid black lines indicate the interface between the polymer layers. The plots show where the electric field intensity is generated within the polymer films as well as waveguide mode angles. (A) Sample 1-Bi: 140 nm PMMA, 180 nm PS; and (B) sample 2-Bi: 296 nm PMMA, 159 nm PS. (C) Sample 1-Tri: 160 nm top PMMA (closest to the prism), 420 nm bottom PMMA (farthest

from the prism); and (D) Sample 2-Tri: 300 nm top PMMA, 310 nm bottom PMMA. The Sample 1-Tri and 2-Tri PS layer thickness is 180 nm. The calculations used a 0.05° step size.

Compared to sample 1-Bi, sample 2-Bi (Fig. 1B) shows an increase in the waveguide mode angle as the PMMA thickness increases to 296 nm and the PS layer thickness decreases to 159 nm. For both the PS and PMMA layers the waveguide mode angle occurs at 55.95°. With the increasing PMMA thickness for sample 2-Bi, there is a decrease in the electric field intensity generated in the PS layer down to 55% compared to the 63% generated in the PS layer for sample 1-Bi.

For the trilayer films shown in Fig. 1C and D, the PS thickness is constant at 180 nm. The total thickness is 770 (1-Tri) and 790 nm (2-Tri). Effectively, the PS layer is farther from the prism interface for sample 2-Tri as the thickness increases for the PMMA layer adjacent to the prism. The trilayer films are thick enough to generate two waveguide modes within this angle range, and they are termed mode zero (at high angles) and mode one (at low angles) as observed in Fig. 1C and D. Fig. S1 (Supporting Information) shows the plots of the calculated electric field intensity as a function of the distance from the prism/sample interface at the PMMA waveguide mode angle for sample 1-Tri, where the purple curve is waveguide mode one (51.95° incident angle) and the orange curve is waveguide mode zero (58.75° incident angle). Similar plots are obtained at the PS waveguide mode angle. The graphs show that the distribution of the electric field intensity among the polymer layers varies with each waveguide mode.

In sample 1-Tri waveguide mode zero appears at 58.75° for both PS and PMMA layers, and waveguide mode one is at 51.85° for PS and 51.95° for PMMA. Compared to sample 1-Tri,

sample 2-Tri waveguide mode zero for PS and PMMA shifts to a higher angle (59.15°), and waveguide mode one for PS and PMMA decreases by 0.95° and 0.85°, respectively. As the PS layer moves further away from the prism interface for sample 2-Tri, there is an 8% increase in the electric field intensity within the PS layer at waveguide mode zero, while there is a 1.5% decrease at waveguide mode one. Similar trends are observed for sample 3-Bi (Fig. S2A (Supporting Information)) and sample 3-Tri (Fig. S3A (Supporting Information)). These representative calculated results suggest it should be feasible to use SA Raman spectroscopy, with a signal that is proportional to the electric field intensity,[31-34,38,42-45] to measure total film thickness as well as the location of polymer interfaces for both bilayer and trilayer films.

Development of a SA Raman method with iterative fitting for analyzing bilayer polymer films

Fig. 2A shows the SA Raman spectra plotted over an incident angle range of 50.0-60.0° for sample 1-Bi, and Fig. 2B shows a plot of the peak amplitude as a function of incident angle for the PS (1001 cm^{-1}, red circles) and PMMA (812 cm^{-1}, blue circles) peaks. A single broad waveguide mode is measured for PS and PMMA, with waveguide mode angles at 54.86 ± 0.02° for PS and 55.58 ± 0.03° for PMMA. The PMMA amplitude at 812 cm^{-1} is 2.1× lower compared to the PS amplitude at 1605 cm^{-1}, which is not due to differences in their Raman cross-section ($\sigma_R = 1.0$) or the amount of PMMA in the film (there is only 1.2× less PMMA compared to PS in the sample). Rather, there is an enhancement in the PS signal in sample 1-Bi with the amplitude being 69% of the total signal collected. This is in agreement with the 63% value from the electric field calculations. Overall, the waveguide mode angles and peak amplitudes follow the trends observed in the electric field intensity plot shown in Fig. 1A.

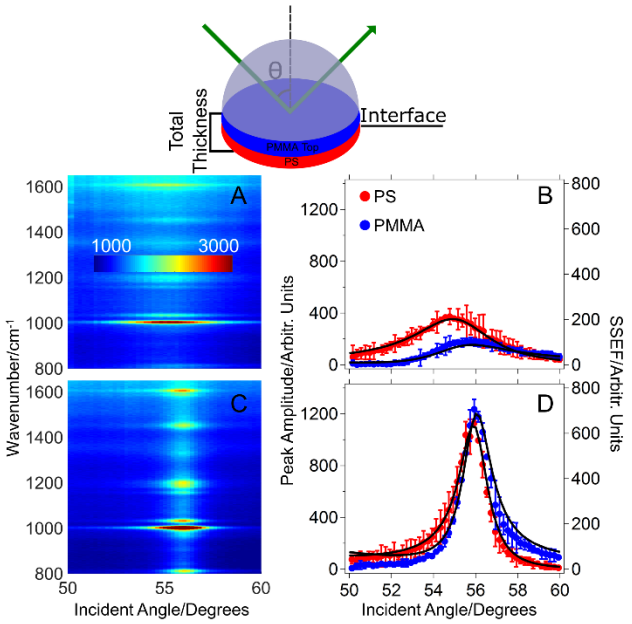

Figure 2: (A and C) SA Raman spectra of PMMA/PS bilayer films plotted on the same color scale shown in A. The color scale represents the SA Raman scattering intensity (Arbitr. Units). (B and D) show plots of the 1605 cm^{-1} PS and the 812 cm^{-1} PMMA peak amplitudes as a function of the incident angle. The black lines represent the best SSEF fit to the experimental data. (A and B) correspond to sample 1-Bi and (C and D) correspond to sample 2-Bi.

SA Raman data for sample 2-Bi (Fig. 2C and D) and 3-Bi (Fig. S2B (Supporting Information)) show the effects of increasing the total thickness. Compared to sample 1-Bi, the PS and PMMA waveguide modes shift to higher angles. The peak amplitudes increase for sample 2-Bi and 3-Bi, and there is an overall decreasing trend in the magnitude of the SA Raman amplitude ratio (r_{PS}) as the PMMA layer thickness increases (Table 1). The SA Raman data are well fit by the iterative SSEF calculations (Fig. 2D and Fig. S2B (Supporting Information)).

Fig. 3 shows the thicknesses measured for each of the bilayer films by SA Raman spectroscopy and by profilometry. Overall, the SA Raman measurements properly capture the increasing PMMA layer thickness, and statistically similar PS thickness for these samples. The interface locations determined by SA Raman spectroscopy (Table 1) are 140 ± 10 (sample 1-Bi), 296 ± 7 (sample 2-Bi), and 440 ± 10 nm (sample 3-Bi). The total thickness and PMMA layer thickness determined by the SA Raman method have an average 4% and 6% difference, respectively, compared to values measured by profilometry. The PS layer thickness has a larger 14% difference compared to the values measured by profilometry. The s_{est} is used to quantitatively determine how well the SSEF calculations fit the experimental SA Raman data. For sample 1-Bi the s_{est} for the best fit to the PS and PMMA data are determined to be 0.043 and 0.052, respectively. The s_{est} of the second-best fit that is shifted by at least 0.2° (the angular resolution of the experimental data) increases to 0.057 and 0.073 (33% and 40% increase) when the total, PS, and PMMA layer thicknesses change by 10 nm as shown in Fig. S4 (Supporting Information). Increasing the angular resolution used to collect the experimental data and/or reducing the thickness increments used in the iterative calculations should improve the average percent difference between the SA Raman method and profilometry measurements at the cost of increased instrumental and computational time. It is also important to note that the samples measured by profilometry are not the same as those measured by the SA Raman method since profilometry is destructive and can only measure the individual layers prior to forming the bilayer.

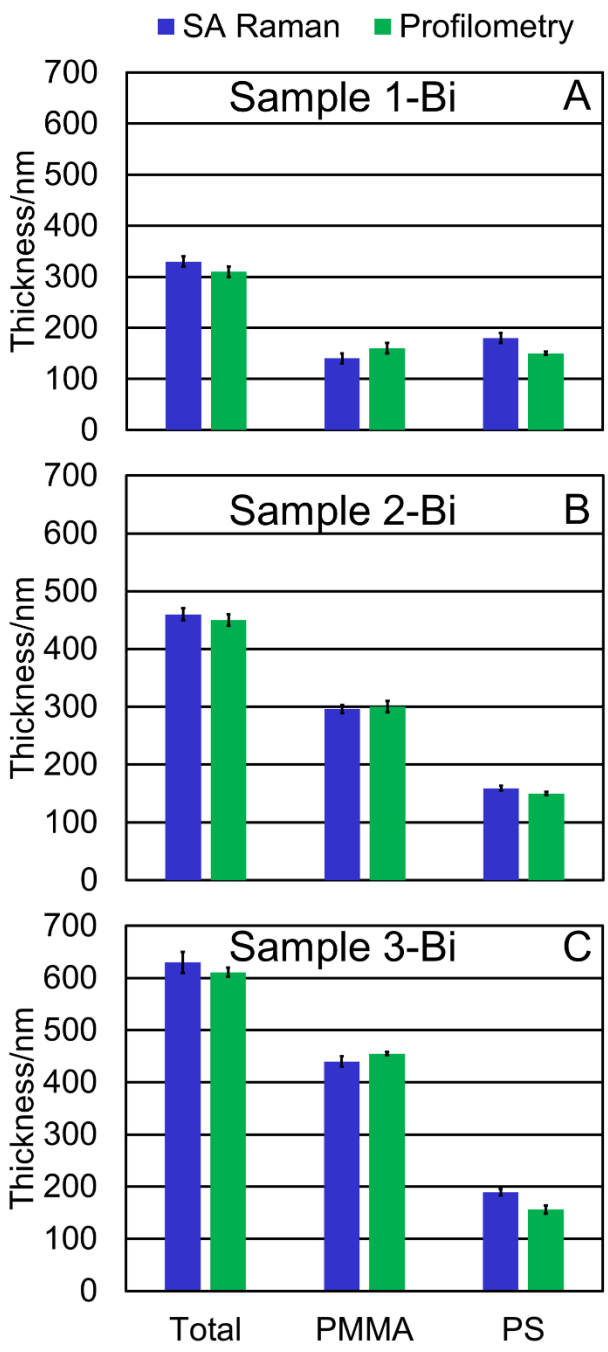

Figure 3: (A) Sample 1-Bi, (B) sample 2-Bi, and (C) sample 3-Bi thicknesses measured by the SA Raman method and profilometry. The profilometry measurements are performed on separate films fabricated with the same method used to prepare the samples measured by SA Raman spectroscopy, and assume the thicknesses measured on the individual layers prior to forming the

bilayer are retained in the bilayer. The error bars represent the difference between the best fit and the second-best fit that is shifted by at least 0.2° for two replicate measurements (SA Raman) and the standard deviation from three replicate measurements (profilometry).

Applying the SA Raman method for analysis of trilayer films

Trilayer films are prepared by transferring a third PMMA layer onto samples 1-Bi and 2-Bi. The corresponding multilayer films are samples 1-Tri and 2-Tri, and their SA Raman spectra are plotted in Fig. 4A and C. The SA Raman spectra for the trilayer films show similar trends to the electric field intensity plots (Fig. 1C and D). Waveguide mode one shifts by 0.9° to lower angles for both PS and PMMA in sample 2-Tri (Fig. 4D) when the PS layer moves farther from the sapphire prism interface. Data for a third trilayer sample (3-Tri) are shown in Fig. S3 (Supporting Information).

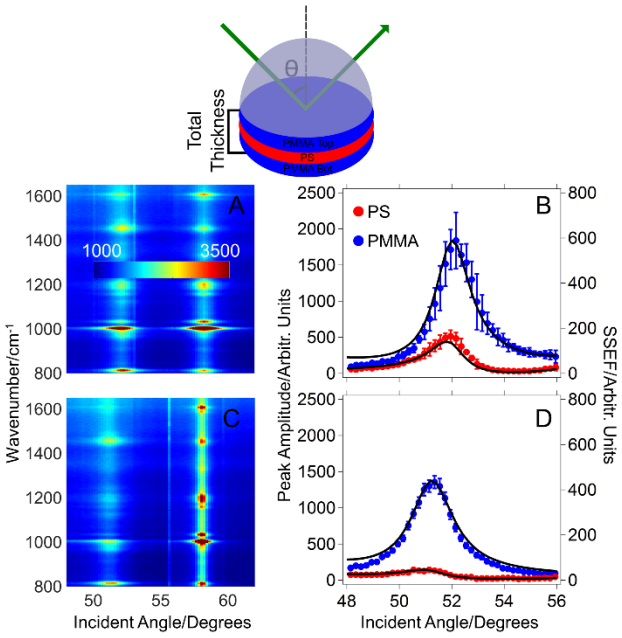

Figure 4: (A and C) SA Raman spectra of PMMA/PS/PMMA trilayer films plotted on the same color scale shown in A. The color scale represents the SA Raman scattering intensity (counts). (B and D) show the plots of waveguide mode one for 1605 cm^{-1} PS and the 812 cm^{-1} PMMA peak amplitudes versus incident angle. The black lines represent the best SSEF fit to the experimental data. (A and B) correspond to sample 1-Tri and (C and D) correspond to sample 2-Tri.

For the trilayer films, waveguide mode one is used to fit the data as better agreement with the profilometry measurement is obtained compared to using waveguide mode zero. This is the result of the smaller angle shifts that occur in thicker films at waveguide mode zero (Fig. 1C and D), and the 0.2° angle resolution used to collect the experimental data. Considering the best instrumental angle resolution of 0.09° and a one micron thick film, the smallest thickness change that can be measured using waveguide mode one is approximately 6 nm. The smallest change in thickness that can be measured using waveguide mode zero is 35 nm since it requires a larger change in the thickness to observe a 0.09° angle shift.

For the trilayer films, the total thickness (1% average difference), top PMMA (6% average difference), PS (15% average difference), and bottom PMMA layer thicknesses (6% average difference) are comparable to the values measured by profilometry as shown in Fig. 5. The layer thicknesses can be used to calculate the two interface locations (Table 1). Since sample 1-Tri and 2-Tri are made by adding a third layer to sample 1-Bi and 2-Bi, the location of the first interface is the same. The location of this interface as measured by SA Raman spectroscopy is statistically similar for the bilayer and trilayer films.

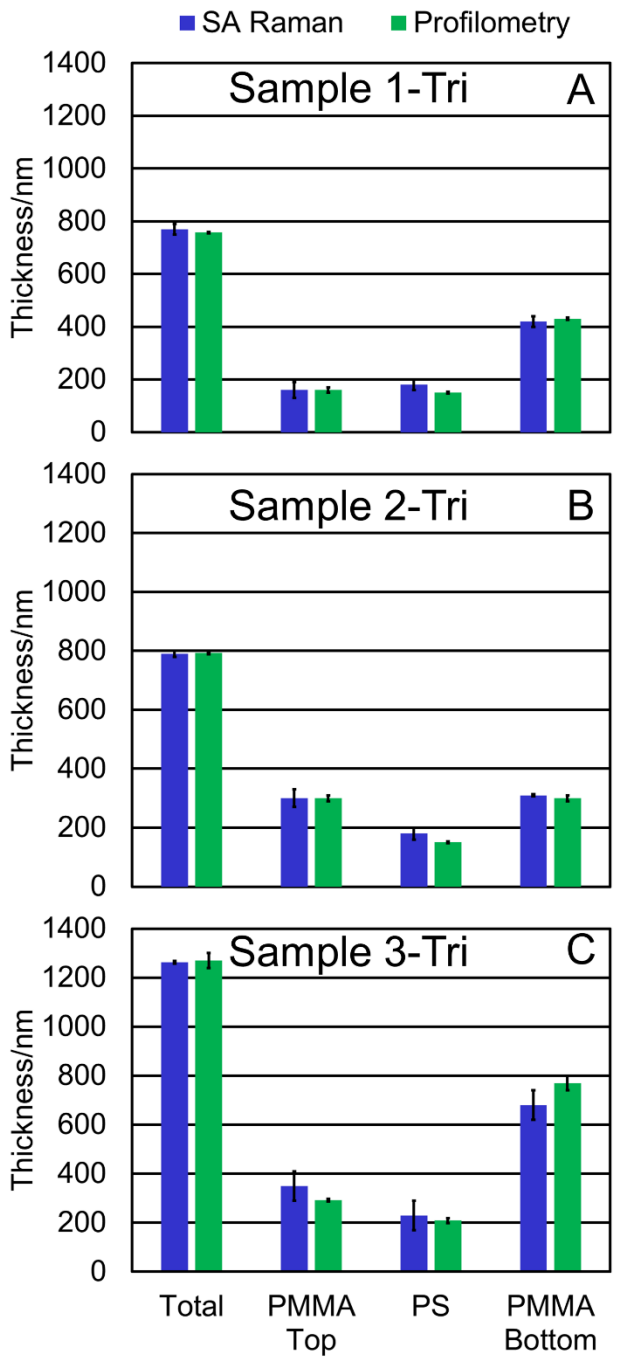

Figure 5: (A) Sample 1-Tri, (B) sample 2-Tri, and (C) sample 3-Tri thicknesses measured by the SA Raman method and profilometry. The profilometry measurements are performed on separate films fabricated with the same method used to prepare the samples measured by SA Raman spectroscopy, and assume the thicknesses measured on the individual layers prior to forming the

trilayer are retained in the trilayer. The error bars represent the difference between the best fit and the second-best fit that is shifted by at least 0.2° (SA Raman) and the standard deviation from three replicate measurements (profilometry).

Conclusion

SA Raman spectroscopy of thin polymer films provides chemical content information about individual layers in intact films, is nondestructive, and requires minimal sample preparation. For PMMA/PS bilayer and PMMA/PS/PMMA trilayer waveguide films total thickness and interface locations are determined by fitting the 812 cm^{-1} PMMA and the 1605 cm^{-1} PS peak amplitude as a function of incident angle with the SSEF calculations. This technique provides chemical content information from multilayer polymer systems with total thicknesses and interface locations with an average 8% (bilayer) and 7% (trilayer) difference when compared to profilometry. This method can be easily applied to a variety of multilayer polymer systems provided each component has at least one distinct Raman peak and a known (or measurable) refractive index and Raman cross section at the excitation wavelength. The SA Raman spectroscopy method of analysis for multilayer polymer waveguide films will be useful for *in situ* measurements for samples ranging from tandem organic/inorganic hybrid energy storage and capture devices to multilayer plastic films used in packaging.

Acknowledgement

This research was supported by the U.S. Department of Energy, Office of Science, Basic Energy Sciences, Chemical Sciences, Geosciences, and Biosciences Division. The research was

performed at Ames Laboratory, which is operated for the U.S. DOE by Iowa State University under contract # DE-AC02-07CH11358.

Appendix A. Supporting Information

The iterative EM Explorer script used to calculate the electric field intensity has been provided. A plot of sample 1-Tri's waveguide mode 0 and mode 1 electric field distribution is shown in Fig. S1 (supporting Information). Samples 3-Bi and -Tri with their corresponding calculated electric field intensity plots, SA Raman spectra, peak amplitude as a function of incident angle plots are provided as Fig. S2 and S3 (Supporting Information). Peak amplitude as a function of incident angle plots with the best fit and the second-best fit are provided for sample 1-Bi and 1-Tri in Fig. S4 (Supporting Information).

References

[1] J.K. Mwaura, M.R. Pinto, D. Witker, N. Ananthakrishnan, K.S. Schanze, J.R. Reynolds, *Langmuir* **2005**; *21*, 10119.

[2] K. Norrman, M.V. Madsen, S.A. Gevorgyan, F.C. Krebs, *JACS* **2010**; *132*, 16883.

[3] S. Fukuta, J. Seo, H. Lee, H. Kim, Y. Kim, M. Ree, T. Higashihara, *Macromolecules* **2017**; *50*, 891.

[4] P. Peumans, S. Uchida, S.R. Forrest, *Nature* **2003**; *425*, 158.

[5] M. Helgesen, R. Sondergaard, F.C. Krebs, *J. Mater. Chem.* **2010**; *20*, 36.

[6] I. Lim, H.T. Bui, N.K. Shrestha, J.K. Lee, S.-H. Han, *ACS Appl. Mater. Interfaces* **2016**; *8*, 8637.

[7] J.Y. Kim, K. Lee, N.E. Coates, D. Moses, T.-Q. Nguyen, M. Dante, A.J. Heeger, *Science* **2007**; *317*, 222.

[8] L. Dou, J. You, J. Yang, C.-C. Chen, Y. He, S. Murase, T. Moriarty, K. Emery, G. Li, Y. Yang, *Nat Photon* **2012**; *6*, 180.

[9] Z. Shao, S. Chen, X. Zhang, L. Zhu, J. Ye, S. Dai, *J. Nanosci. Nanotechnol.* **2016**; *16*, 5611.

[10] T. Fujinami, M.A. Mehta, M. Shibatani, H. Kitagawa, *Solid state Ion.* **1996**; *92*, 165.

[11] S.A. Jenekhe, D.J. Kiserow, *Chromogenic phenomena in polymers: tunable optical properties*, ACS Publications, **2004**.

[12] Z. Wu, J. Walish, A. Nolte, L. Zhai, R.E. Cohen, M.F. Rubner, *Adv. Mater.* **2006**; *18*, 2699.

[13] T. Komikado, A. Inoue, K. Masuda, T. Ando, S. Umegaki, *Thin Solid Films* **2007**; *515*, 3887.

[14] H. Lee, M.L. Alcaraz, M.F. Rubner, R.E. Cohen, *ACS Nano* **2013**; *7*, 2172.

[15] C.-T. Chen, T.-W. Tsai, *Sens. Actuators A Phys.* **2016**; *244*, 252.

[16] E. Canellas, M. Aznar, C. Nerin, P. Mercea, *J. Mater. Chem.* **2010**; *20*, 5100.

[17] S. Alix, A. Mahieu, C. Terrie, J. Soulestin, E. Gerault, M.G.J. Feuilloley, R. Gattin, V. Edon, T. Ait-Younes, N. Leblanc, *Eur. Polym. J.* **2013**; *49*, 1234.

[18] V. Siracusa, C. Ingrao, A. Lo Giudice, C. Mbohwa, M. Dalla Rosa, *Food Res. Int.* **2014**; *62*, 151.

[19] G.K. Such, A.P.R. Johnston, F. Caruso, *Chem. Soc. Rev.* **2011**; *40*, 19.

[20] W.-K. Lee, J.-H. Ryou, W.-J. Cho, C.-S. Ha, *Polym. Test.* **1998**; *17*, 167.

[21] P. Müller-Buschbaum, J.S. Gutmann, J. Kraus, H. Walter, M. Stamm, *Macromolecules* **2000**; *33*, 569.

[22] Z. Zhang, D.U. Ahn, Y. Ding, *Macromolecules* **2012**; *45*, 1972.

[23] Q. Yang, Y. Zhu, J. You, Y. Li, *Colloid. Polym. Sci.* **2017**; *295*, 181.

[24] S. Kang, V.M. Prabhu, C.L. Soles, E.K. Lin, W.-l. Wu, *Macromolecules* **2009**; *42*, 5296.

[25] I. Erel-Unal, S.A. Sukhishvili, *Macromolecules* **2008**; *41*, 8737.

[26] S. Owusu-Nkwantabisah, M. Gammana, C.P. Tripp, *Langmuir* **2014**; *30*, 11696.

[27] T.T.M. Ho, K.E. Bremmell, M. Krasowska, S.V. MacWilliams, C.J.E. Richard, D.N. Stringer, D.A. Beattie, *Langmuir* **2015**; *31*, 11249.

[28] T. Jawhari, J. Pastor, *J. Mol. Struct.* **1992**; *266*, 205.

[29] S. Qin, D. Qin, W.T. Ford, Y. Zhang, N.A. Kotov, *Chem. Mater.* **2005**; *17*, 2131.

[30] N.J. Everall, *Appl. Spectrosc.* **2000**; *54*, 1515.

[31] W.M. Matthew, H.T.N. Vy, A.S. Emily, *Vib. Spectrosc* **2013**; *65*, 95.

[32] M.W. Meyer, K.L. Larson, R.C. Mahadevapuram, M.D. Lesoine, J.A. Carr, S. Chaudhary, E.A. Smith, *ACS Appl. Mater. Interfaces* **2013**; *5*, 8686.

[33] C.A. Damin, V.H. Nguyen, A.S. Niyibizi, E.A. Smith, *Analyst* **2015**; *140*, 1955.

[34] J.M. Bobbitt, D. Mendivelso-Pérez, E.A. Smith, *Polymer* **2016**; *107*, 82.

[35] N. Fontaine, T. Furtak, *Phys. Rev. B: Condens. Matter* **1998**.

[36] I. Fumihiko, K. Munsok, *Jpn. J. Appl. Phys.* **2008**; *47*.

[37] G.F. Schneider, V.E. Calado, H. Zandbergen, L.M.K. Vandersypen, C. Dekker, *Nano Lett.* **2010**; *10*, 1912.

[38] M.D. Lesoine, J.M. Bobbitt, S. Zhu, N. Fang, E.A. Smith, *Anal. Chim. Acta* **2014**; *848*, 61.

[39] M. Bass, C. DeCusatis, J. Enoch, V. Lakshminarayanan, G. Li, C. Macdonald, V. Mahajan, E. Van Stryland, *Handbook of optics, Volume II: Design, fabrication and testing, sources and detectors, radiometry and photometry*, McGraw-Hill, Inc., **2009**.

[40] S.N. Kasarova, N.G. Sultanova, C.D. Ivanov, I.D. Nikolov, *Opt. Mater.* **2007**; *29*, 1481.

[41] N. Sultanova, S. Kasarova, I. Nikolov, *Acta Phys. Pol., A* **2009**; *116*, 585.

[42] K. McKee, E. Smith, *Rev. Sci. Instrum.* **2010**; *81*, 43106.

[43] W.M. Matthew, J.M. Kristopher, H.T.N. Vy, A.S. Emily, *J. Phys. Chem. C* **2012**; *116*.

[44] K. McKee, M. Meyer, E. Smith, *Anal. Chem.* **2012**; *84*, 9049.

[45] K. McKee, M. Meyer, E. Smith, *Anal. Chem.* **2012**; *84*, 4300.

Table 1: The experimental SA Raman amplitude ratios (r_{PS}) and interface locations determined by SA Raman spectroscopy.

Sample	Total Thickness Range Used in Calculation (nm)	Measured SA Raman Amplitude Ratio (r_{PS}) Range Used in Calculation	Measured Interface 1 (nm)	Measured Interface 2 (nm)
1-Bi	300-360	0.4-0.8	140 ± 10	NA
2-Bi	420-480	0.3-0.7	296 ± 7	NA
3-Bi	600-660	0.2-0.6	440 ± 10	NA
1-Tri	740-800	0.1-0.3	160 ± 30	340 ± 40
2-Tri	740-800	0.08-0.23	300 ± 30	480 ± 40
3-Tri	1230-1290	0.12-0.22	350 ± 60	580 ± 80